Final Report

Title: Semiconductor detectors with proximity signal readout

(Topic 45/b)

Company	XIA LLC
Principal Investigator	Dr. Stephen J. Asztalos
Address:	31057 Genstar Rd, Hayward, CA 94544
Grant Award Number	DE-0006317
Date	04/14/2012
Reference number	DE-FOA-0000676
Topic	45b. Position sensitive detectors

This document contains no proprietary technical information and can be made available to the general public

1 Phase I Technical Report

1.1 Overall Technical Objective

The technical feasibility of our Phase I work goals was demonstrated by meeting all and exceeding some of our initial objectives. Below we summarize the work done in accomplishing our Phase I objectives by demonstrating position-sensitive readout of HpGe detectors. We then exceeded our goals

by reconstructing position and energy information as part of a detailed characterization of the detector performance.

1.2 Executive Summary

Semiconductor-based radiation detectors are routinely used for the detection, imaging, and spectroscopy of x-rays, gamma rays, and charged particles for applications in the areas of nuclear and medical physics, astrophysics, environmental remediation, nuclear nonproliferation, and homeland security. The types of radiation that can be measured with semiconductor detectors include a large portion of the electromagnetic spectrum, with photon energies ranging from <1 eV (near infrared) to ~10 MeV (gamma rays), and charged particles with energies from keV to GeV. Detectors used solely for determining the presence, intensity, and energy of a radiation source can be relatively simple, and typically consist of a single piece of semiconductor onto which two electrodes have been fabricated. These electrodes are used for bias voltage application and signal readout. Well established and reliable technologies exist for the manufacture of such detectors. An example of this type of detector is the high-purity Ge (HpGe) coaxial gamma-ray detector that is considered the gold standard for gamma-ray spectroscopy.

In contrast to the simple single element spectroscopy detectors, detectors used for imaging and particle tracking are more complex in that they typically must also measure the location of the radiation interaction in addition to the deposited energy. In such detectors, the position measurement is often achieved by dividing or segmenting the electrodes into many strips or pixels and then reading out the signals from all of the electrode segments. Fine electrode segmentation is commonly done on wafer thickness Si devices that are manufactured using high process temperatures but is problematic for many of the standard semiconductor detector technologies. This includes HpGe and lithium-drifted Si (Si(Li)) based detectors. The lack of a good passivating oxide on Ge and the process temperature limit of Si(Li), which precludes the use of a thermal oxide, means that isolation between electrode segments cannot simply be achieved through a native oxide as is done for a conventional Si device. Additionally, Li diffusion is the basis for one of the standard electrodes on these detectors, and Li readily diffuses in Ge and thereby limits the granularity of the electrode segmentation to no better than 1 mm. Detector electrodes based on amorphous-semiconductor layers have in part been able to address these limitations, but the technology still requires additional development in order to minimize leakage current, reduce sensitivity to temperature cycling, and improve robustness[1].

In addition to the challenges of fabricating a position-sensitive detector is the challenge of connecting to all of the electrodes on such a detector. The electrical connection to the detector can be done through spring-loaded pins, wire bonding, or bump bonding. The pin approach is limited to coarse electrode segmentation and can damage the fragile detector electrodes. Wire bonding is commonly used but is not appropriate for densely packed structures such as finely pixilated detectors and must be carefully done when directly bonding to the active areas of the detectors (as is typically the case for HpGe detectors). Bump bonding in which an intermediate board with electrical interconnection traces is bonded to the detector through soft metal bumps is a technology that has been used for finely pixilated detectors. This approach however is not straight-forward for detectors that must be cryogenically cooled such as those based on HpGe. Differential thermal contraction between the detector and bonded board can lead to bond failure and detector damage.

A final challenge associated with a position-sensitive detector is reading out the signals from all of the electrodes. The positional accuracy obtained with the detector is normally given by the spacing between the electrodes. As such, to achieve a better resolution, a greater number of electrodes and, consequently, channels of readout electronics are required. High channel densities are costly, have high

power requirements, and can be difficult to design and manufacture (particularly with cryogenic detectors such as HpGe where the detector must be contained within a vacuum enclosure).

There clearly is a need for a detector technology that can achieve fine position resolution while maintaining the excellent energy resolution intrinsic to semiconductor detectors, can be fabricated through simple processes, does not require complex electrical interconnections to the detector, and can reduce the number of required channels of readout electronics. The proximity electrode signal readout technology satisfies this need [2]. With this technology, the signal readout is accomplished by measuring the charge induced on electrodes positioned close but not electrically connected to the semiconductor detector material. These electrodes are fabricated onto a circuit board that is positioned a small distance from the surface on the detector onto which charge is collected. The electrode complexity is then no longer a problem associated with the detector fabrication, but is one that is easily dealt with using well established and inexpensive circuit board manufacturing processes. When compared to conventional position-sensitive detectors, this approach significantly simplifies the electrodes electrically connected to the detector, which are still necessary for bias voltage application and charge collection.

The proximity readout technique offers the advantages of simplified detector fabrication (as described above), expanded electrode geometry options, and improved position detection through signal interpolation. The options for electrode geometries are greater because the electrodes no longer need to be placed on a single plane. For example, a multilayer circuit board can be used to create an orthogonal strip electrode configuration that is implemented using only one side of the detector for signal readout. The substantial benefit of improved position detection is made possible by the fact that the charge is not fully collected to any one proximity electrode. Instead, the charge from a radiation interaction event is collected to the detector surface and induces charge on the proximity electrodes in an amount determined by the electrode geometry and position relative to the radiation-generated charge. Since multiple electrodes will have non-zero integrated signals, simple interpolation (or other similar calculations) can be used to achieve a position resolution much finer than the electrode spacing.

In Phase I of this program, our primary objective was to build and demonstrate cryogenically-cooled HpGe detectors with proximity charge sensing signal readout. To achieve this objective, a cryostat was fabricated along with the necessary readout electronics, detector fabrication processes were evaluated and applied to make proximity detectors, and detailed characterization of the detectors along with extensive data analysis were completed. All aspects of the program were successfully completed, and a clear demonstration of the proximity approach, as applied to HpGe, was made. Two prototype detectors were produced and evaluated. Both gamma-ray position (finer than the electrode spacing) and energy determination were demonstrated with these detectors.

The primary objective for Phase II of this program is to further demonstrate and explore the advantages of the proximity readout technique as applied to HpGe gamma ray detectors.

The success of our Phase I work was critically dependent on the performance of the a-Ge proximity surface as two competing requirements had to be met simultaneously: electric field transparency and efficient charge dissipation. We encountered immediate success in this regard - it was found that a-Ge sputtered in a mixture of Ar and H_2 had an acceptable resistivity level to function properly as the proximity surface coating. Encouraged by this work we then went further to extract position and energy information from these data. Pulse-height event data sets were acquired from these detectors using a variety of gamma-ray sources. Two different reconstruction methods were employed to determine the position and energy resolution; one based on calculated weighting potentials, the other based on experimentally reconstructed weighting potentials. Here we enjoyed further success by demonstrating

sub pixel resolution directly from the signals. These results give us high confidence in the success of our proposed Phase II work.

We now summarize our Phase I work plan: two small HpGe strip detectors approximately 10 mm thick and 18 x 18 mm^2 in area were fabricated for this work. The on-detector electrodes consist of a full-area amorphous Ge (a-Ge)/Al contact on one side and a full-area a-Ge with two edge Al strips on the opposing (proximity) detector surface (see Error: Reference source not foundb). These on-detector electrodes were used for bias voltage application and charge removal. The proximity electrodes geometry measured 1 mm in width and strips with a 2 mm pitch (5 total) suspended approximately 50 μm above the proximity detector surface. I-V curves were recorded and low leakage current was exhibited. A cryostat was repurposed for our measurements with modifications restricted mainly to the design of detector mount and IR shield. Lead wires from the proximity electrodes were run from a cryogenic feedthrough and terminated on the input terminal of the preamplifier board mounted on the cryostat. The amplified signals were feed to two XIA Pixie-4 digital spectrometers. Waveforms stored in the list mode data were written to disk and all analyses were performed offline. These data represented the successful culmination of our Phase I project.

The following sections of this Chapter provide a detailed summary of the technical work completed in Phase I. This report is aligned with the five technical objectives specified in our Phase I proposal: (1) Cryostat redesign, construction, and testing, (2) Readout electronics construction and testing, (3) Detector development, (4) Integration and preliminary testing, and (5) Detailed characterization and data analysis.

Objective 1: Cryostat redesign, construction, and testing

The goal of this objective was to retrofit an existing cryostat in order to accommodate the new detection system being developed. Sub-tasks included modifying feedthroughs to achieve reduced noise levels, design of new detector mounting hardware, and fabricating parts for mounting of electronics. These tasks were completed as planned and other difficulties were addressed as they presented themselves.

Task 1.1 - Main cryostat body modifications

The larger pieces of the cryostat are from a previous system that LBNL had in their possession. The cryostat is of a traditional dipstick design. They main body has a 6.875” radius cylindrical cavity with various feed-through ports for electrical readout and monitoring, as well as vacuum ports. The existing electrical feedthroughs were not designed for low noise application, so new ports were machined to mount an ISO type, K16 flange with a 9-pin, C-type, glass electrical feed-through (commercially available through Ace-Glass Products, Inc.). Additional tapped holes were machined for mounting of a spacer needed to gain clearance for the preamplifier electronics box. Since the signal feed-through was the only one required to maintain low noise, existing ceramic electrical feedthroughs were used for thermometry and high voltage. See Figure for before and after SolidWorks renderings of the main cryostat body modifications.

(a) 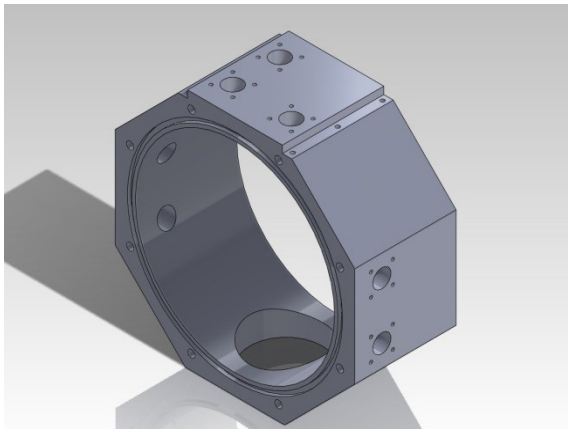 (b) 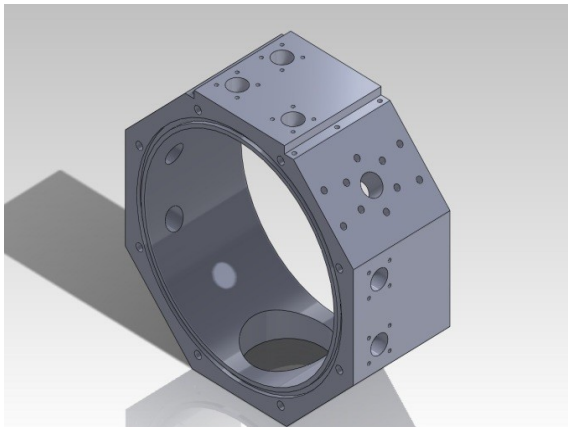

Figure Before (a) and after (b) renderings of main body modifications. Note that visible, modified geometries are mirrored about a vertical, bisecting plane (i.e. the new hole pattern also exists on the opposing, top, diagonal face). This additional feed-through was not needed initially and was covered with a blank ISO flange.

Task 1.2 - Design and fabrication of mounting setup

An existing preamplifier box, previously used for a double sided strip detector, was employed for preamplifier power and outputs. A spacer was made in order to mount the box and have space to run connections to the feed-through. The spacer was designed to mount over the bulkhead clamp for the electrical feed-through and bolt directly to the main cryostat body. The preamplifier box mounts on top of the spacer, and a faceplate is bolted on such that the inside is fully sealed to outside electrical noise sources. Figure shows a SolidWorks rendering of the setup.

(a) 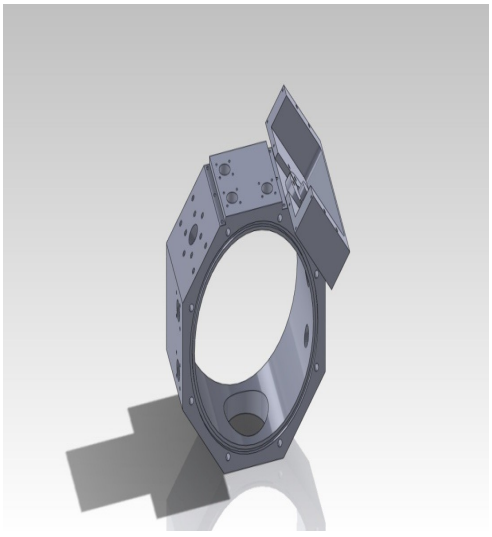 (b) 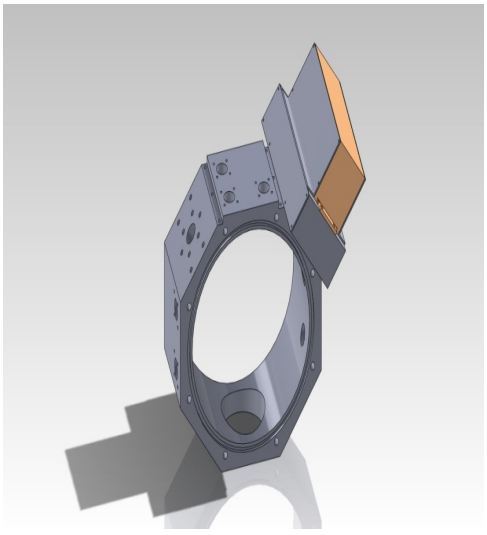

Figure Preamplifier mount and associated face plates.

Task 1.3 - Cold finger mounting

To cool the detector to near liquid nitrogen temperatures, a mounting system was designed to attach to the cold finger. The system consisted of a clamp and a plate on which detector mounts could be bolted. Indium foil was used to ensure good thermal contact between the parts. The detector mounting

plate was designed with additional tapped holes for thermometry, high voltage (HV) feedthrough, and other electrical mounting. These components can be seen in Figure .

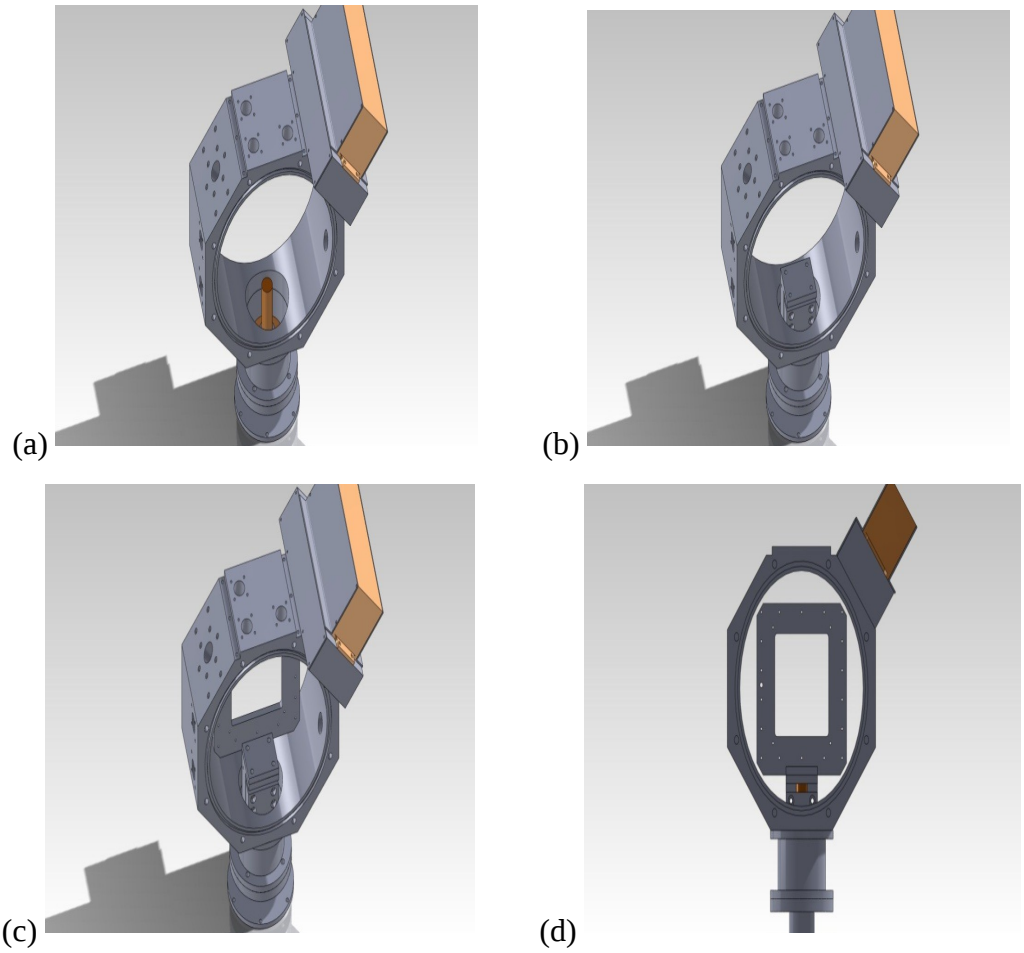

Figure Cold finger mounting system. (a) Copper cold finger. (b) Cold finger clamp. (c) Detector mounting plate. (d) Alternate view of detector mounting plate.

Task 1.4 - Detector mounting

A crystal mount was designed to attach to the cold plate and hold the detector crystal along with the necessary electronics. The main geometries for crystal mounting were based on a previous LBNL design intended for use with the crystal geometries being used. An infrared (IR) shield was also designed for use with this mount. Since electrical feedthroughs into the mount were required, a Teflon connector was fabricated, thereby completing the IR shield. Indium foil was used to ensure good thermal contact where electrical conductivity between parts was not an issue. For thermal contact to the detector crystal, boron nitride was used, to keep the crystal wings electrically insulated from the grounded mount. Tapped holes in the mount were used for crystal mounting, proximity board mounting, and electrical connections (discussed in the electrical work section). A SolidWorks rendering of the mount and IR shield can be found in Figure .

(a) 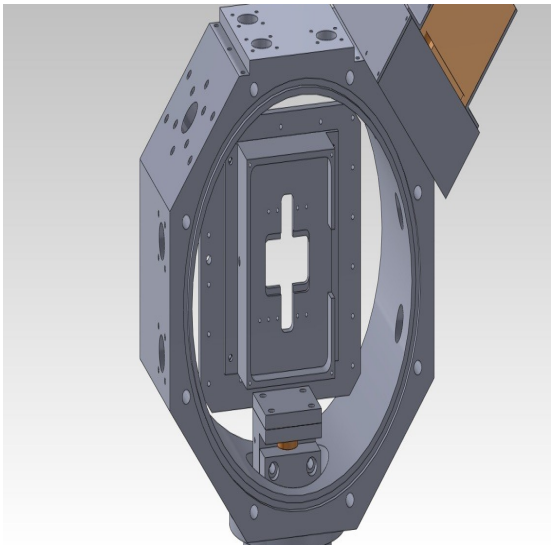 (b) 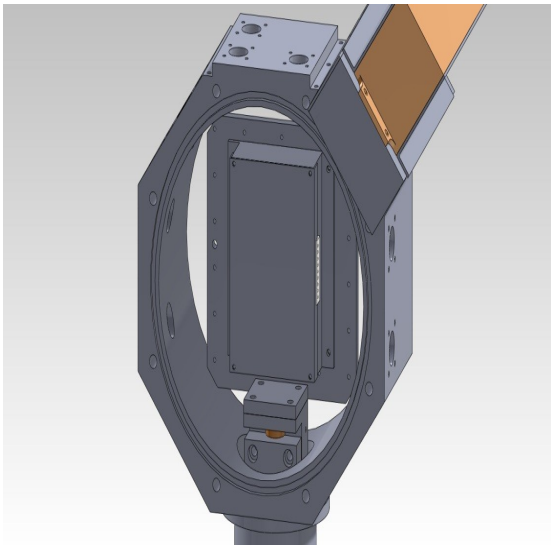

Figure Detector mount without and with the IR shield.

Task 1.5 - Cryostat face plate modification

To allow for detector scanning, the former, thick face plates were redesigned with a thin window. Detector scanning was also the purpose for adding the square hole in the cold plate (shown in Figure). The thin window on the new face plate is 0.02” thick and is shown in Figure .

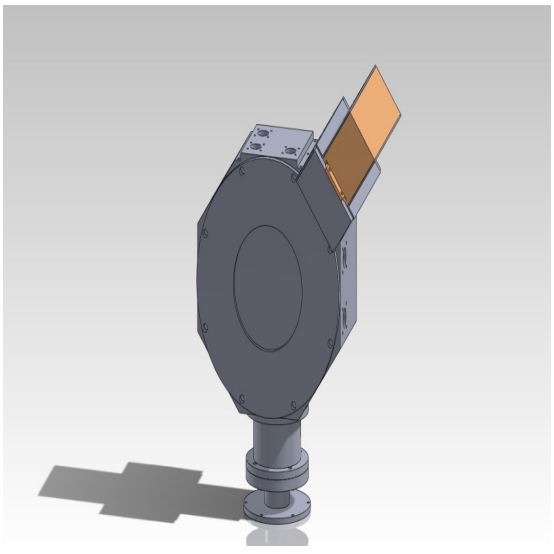

Figure Cryostat face plate with thin window.

Task 1.6 -Thermometry

A commercially available silicon diode thermometer was mounted on the back of the cold plate. A resistance heater was also mounted to the cold plate, near the bottom to flatten temperature gradients near the crystal when heating. This heater allows the user to operate the detector at various temperatures. This variable temperature nature is useful for detector characterization, and, in this

particular case, for charge clearing from the bottom amorphous contact (discussed in a later section). The leads for these components were routed out through an existing ceramic feedthrough and connected to a Lakeshore temperature controller.

Task 1.7 - Modified cryostat testing

Before mounting the detector for measurements, the modified system was thoroughly He leak checked to make certain that sealing surfaces were intact. The baseline vacuum and cold plate temperature were then checked to see they would meet the system requirements. The baseline temperature was ~83K with no detector mounted (Note: the temperature achieved with a detector mounted was only slightly higher than without; i.e. ~84K). The cryosorption material was then regenerated while connected to a turbo pump and the pressure achieved was in the mid 10^{-7} Torr. The system was then ready for detector measurements.

Objective 2: Improve readout connections and preamplifiers

The goal of this objective was to design and assemble the electronics needed for signal readout as well as for system monitoring. Subtasks included assembling preamplifiers and associated passive components, thermometry electronics, and high voltage electronics. These tasks were all completed successfully.

Task 2.1 - Electrical contacts associated with the detector mount

Electrical connections inside the detector mount are all routed from a Teflon feed-through (that completes the IR shield), with the exception of the high voltage. There are five sensing strips, two edge strips (used for HV application and charge removal), and a HV wire. All of these are depressed onto the detector with electrically insulated spring wire. The strips are on a printed circuit board to which wires are soldered. These wires then route to the Teflon feed-through. The HV feed-through is a modified Teflon screw through which an insulated wire is fed. There are solder joints at either end of this feed-through.

Task 2.2 - Preamplifiers and preamp housing

A preamplifier box, formerly used for a double sided strip detector, was re-purposed for use with the proximity detector. The box is powered with ±12VDC which is filtered and distributed via a NIM module. The preamplifiers plug into six pin sockets, where they get their power and output an amplified signal to an SMA connector. Five preamps were tested to ensure low noise operation, and passive components were soldered in to provide pulsing capabilities. The preamps are of a LBNL design which has been iterated at Lawrence Livermore National Laboratory, and are made to couple well with high capacitance detectors. Connections to the two “guard ring” edge strips (see Task 3 section) are also contained in the preamp box but are routed directly to the SMA connectors. This allows for voltage application to the edge strips, however, these are normally grounded.

Task 2.3 – Pixie-4 and Igor data acquisition program

XIA’s commercially available PIXIE-4 was used as the data acquisition system. The modules resided in a National Instruments 1033 5-slot crate. As described in Section Error: Reference source not found, the Pixie-4 is a four channel, 75MHz 14-bit spectrometer operated through an Igor based (Wavemetrics) graphical user interface, also programmed by XIA. A total of five proximity electrodes were read out, hence two Pixie-4 modules were required. Triggers were distributed between modules by connecting the module's trigger signals to the chassis backplane. The rise time we used for the trapezoidal filter was 13.227 us and the flat top was 0.320 us. The count rate varied widely with the

different geometries and sources used. For flood illumination with a ~10 uCi Co-57 source the event rate was approximately 1000 cps. With a collimated Am-241 source (~10mCi) the event rate was about 100 cps. In Section Error: Reference source not found we also discuss the need to move away from the Pixie-4 and pursue a high density electronics solution instead.

Task 2.4 - High voltage feedthrough

A commercially available electronics box was modified for mounting on the outside of the cryostat, over the ceramic HV feed-through. This box has a SHV connector for HV application and a BNC connector for a pulser. The passive circuit inside is a high voltage, low pass filter with a pulser input built in. The circuit is mounted on a Teflon platform to reduce vibration.

Objective 3: Detector development

The goal of this task was to produce small prototype HpGe-based gamma-ray detectors that rely on proximity strip electrodes for signal readout. We selected and tested HpGe samples as conventional (planar) detectors, evaluated the fabrication recipes appropriate for the production of the proximity detectors, and, finally, produced the prototype detectors using the selected HpGe samples and evaluated fabrication process. Two proximity readout detectors were successfully produced. The details of the detector development are provided immediately below. The results obtained with the detectors are described under Objective 5.

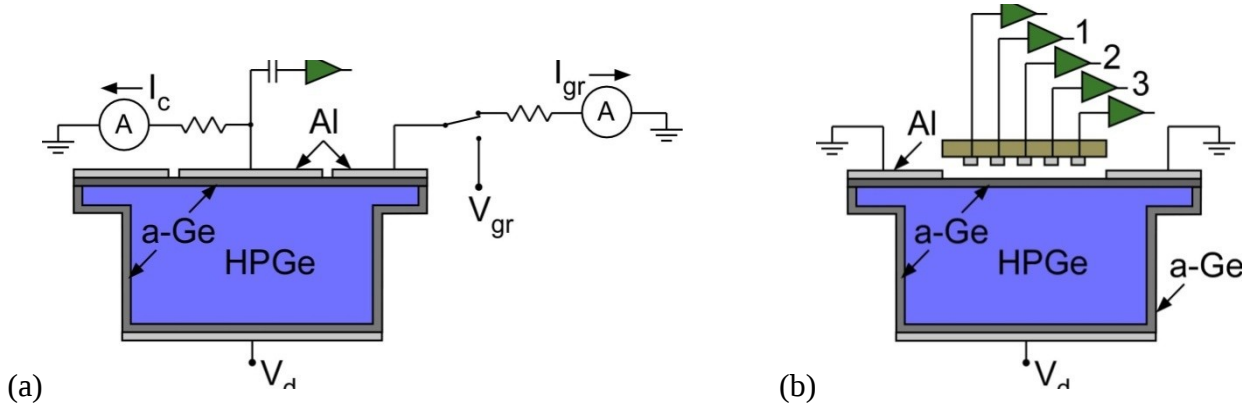

Figure Schematic drawings of (a) the guard ring test configuration used to evaluate the HpGe samples and fabrication process and (b) the HpGe-based proximity readout detectors used in our study.

Task 3.1 - HpGe selection and fabrication process evaluation

HpGe crystals were selected from a supply of existing material at LBNL. The crystals were cut to produce an active detector volume approximately 10 mm thick and 18 x 18 mm^2 in area. The geometry includes two wing regions that remain undepleted during operation and facilitate handling during detector processing and eventual attachment of the detector to its mount (see Figure). Following this mechanical processing, the samples were fabricated into conventional planar detectors of a configuration with separate center and guard ring electrical contacts on the low-voltage side of the detector (see Figure a). This guard ring configuration is important for device diagnostics as it allows the bulk injected leakage current to be measured separately from that flowing along the surface of the detector.

The detector fabrication process used for the initial HpGe sample testing employed (a-Ge) electrical contacts. This contact technology was invented and has been extensively studied at LBNL. The recipe for the deposition of the a-Ge for this project was one in common use for making strip detectors at

LBNL and consisted of sputtering the a-Ge in a gas mixture of Ar and H_2. The a-Ge film created with such a process is referred to here as a-Ge(Ar, H_2). Following the a-Ge(Ar, H_2) sputter deposition over the entire detector surface, select areas were coated with Al using thermal evaporation. The Al areas define the electrical contact areas and were used for voltage bias application and signal measurement. The completed detectors were then loaded into an existing variable temperature cryostat (see Figure) and cooled in preparation for basic electrical testing.

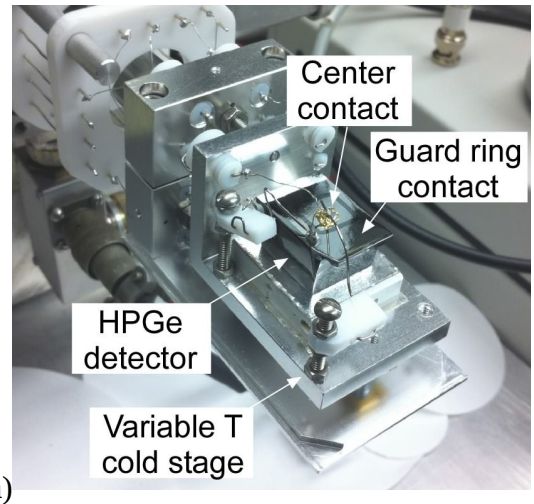

(a)

Figure HpGe guard-ring detector loaded into a variable temperature cryostat in preparation for electrical testing.

The electrical contact configuration used for the testing of the HpGe guard-ring detectors is shown in Figure a. Standard leakage current (both guard ring, I_{gr}, and center contact, I_c) as a function of detector voltage, and capacitance as a function of detector voltage (C-V_d) measurements were made. The C-V_d measurement is used to determine the full depletion voltage, and the I-V_d measurements indicate if the detector can operate at a desired low level of leakage current (~ 10 pA or less). The leakage currents can depend significantly on temperature. For this reason, the measurements were typically made at several temperatures so as to cover the range of possible operating temperatures expected in the proximity cryostat.

Two samples were selected and evaluated. Both functioned well with low leakage current. Additional details are given in the table below.

Sample	Full depletion voltage (V)	Impurity concentration (cm^{-3})	Impurity type
HP40948-3B	1500	2.7×10^{10}	p
313-3.8	300	5.3×10^{9}	n

Table Properties of the HpGe crystals used in the proximity detector study.

Following the detector testing with the detectors fabricated using a standard a-Ge recipe; the crystals were reprocessed using recipes appropriate for the proximity readout configuration. The properties of the a-Ge coating on the proximity surface are critical to the functioning of the detector. Charge is generated by gamma-ray interaction events in the detector volume, then is collected to this surface and is sensed by the proximity strip electrodes, which are positioned just above the surface. For charge to be effectively induced on the proximity electrodes, the a-Ge must

be transparent to the field of the radiation-generated charge but still conductive enough that the collected charge eventually drains to the on-detector edge contacts. Based on our previous work, we anticipated that a-Ge sputtered in pure Ar (referred to as a-Ge (Ar)) would provide an acceptable resistivity to function properly as the proximity surface coating. A-Ge also was used as a passivating coating on the sides of the detector. The proximity surface a-Ge(Ar) recipe however is not appropriate for this purpose since the low resistivity of the film would result in an undesirably high leakage current when the detector voltage is applied. Consequently, the sides as well as the high voltage contact side of the detector used an a-Ge(Ar, H_2) recipe.

The reprocessed HpGe crystals were of a guard-ring configuration as before and were evaluated using I-V_d measurements. Both detectors, again, functioned well. In addition to the I_{gr}-V_d and I_c-V_d measurements, I_c-V_{gr} characteristics were acquired. These characteristics provide a measure of the a-Ge(Ar) sheet resistance, which, as described above, is an important property for the proper operation of the proximity detector. Sheet resistances of the a-Ge(Ar) film on the HP40948-3B detector are listed in. The values range from about 10^{10} to 10^{11} ohm/square. This is a bit higher than desired, but is acceptable.

Temperature (K)	Detector voltage (V)	Sheet resistance (Gohm/square)
79.2	1000	93.5
90	1000	32.4
100	1000	14.4

Table Extracted sheet resistance measured on the HP40948-3B guard-ring detector at several temperatures.

Task 3.2 - Proximity detector production

Once the fabrication process was confirmed to produce guard-ring detectors with the desired properties, the two HpGe crystals were reprocessed into proximity readout detectors of the geometry schematically shown in Figure b. The detector configuration was such that the electrical contacts used for bias voltage application and charge removal consisted of a full-area a-Ge(Ar, H_2)/Al contact on one side and a full-area a-Ge(Ar) film with two Al edge strips (guard strips) on the opposing (proximity) detector surface. The proximity electrodes were 1 mm wide strips at a 2 mm pitch, positioned approximately 50 μm above the proximity detector surface.

Objective 4: Integration and preliminary testing

The goal of this task was to integrate all components developed as part of Tasks 1-3 (cryostat, electronics, and proximity detector) into a complete system, debug and correct any issues, and then perform preliminary detector testing. No issues were encountered in the system integration. Photographs documenting the detector assembly sequence are given in Figure . The completed detector package loaded into the test cryostat is shown in Figure .

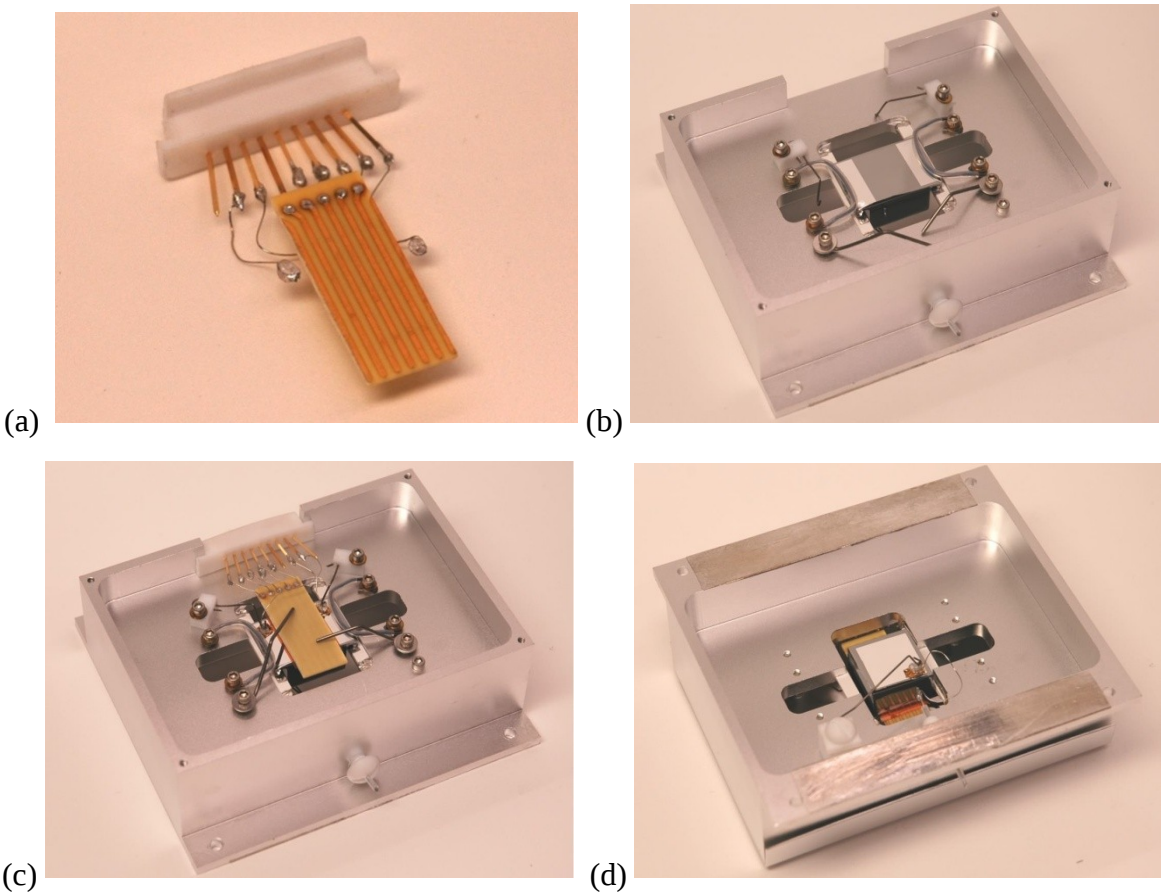

Figure Proximity readout detector assembly. (a) Detector loaded into the detector mount. (b) Proximity readout board and connector assembly. (c) Proximity readout side of completed detector assembly. (d) High-voltage side of completed detector assembly.

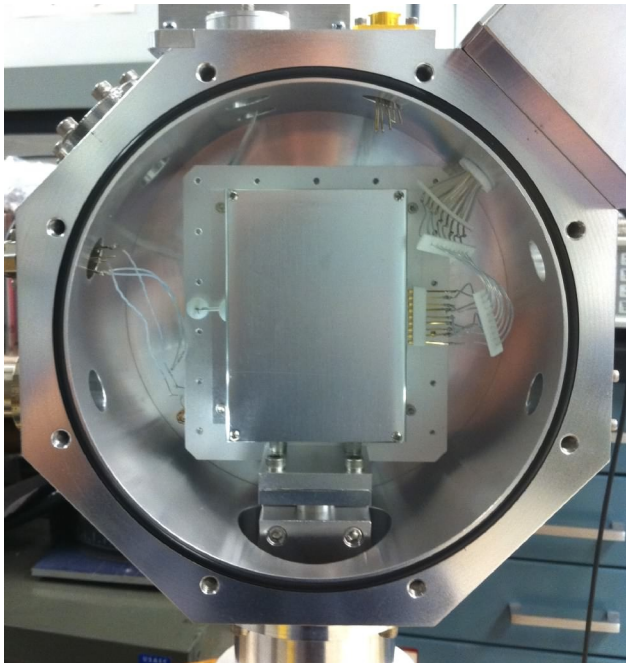

Figure Proximity detector assembly loaded into the test cryostat.

The preliminary testing of the proximity detectors included electrical and simple qualitative radiation response measurements. The electrical measurements consisted of current-voltage (I-V) characteristics measured across the detector and between the two guard strips. As before the I-V characteristics across the detector were used to determine if the detectors functioned properly. This requires operating above full depletion at a desired low level of leakage current. Both HP40948-3B and 313-3.8 met this requirement. Shown in Figure Current-voltage characteristics measured from the HP40948-3B proximity readout detector at the temperatures of 84 and 90 K. (a) Characteristics measured across the detector. (b) Characteristics measured between the two guard strips when 2000 V was applied across the detector.a are example measurements made on HP40948-3B. The I-V characteristics measured between the two guard strips provide a measure of the a-Ge(Ar) sheet resistance. Sheet resistances of order 100 Gohms/square were obtained with the two detectors. Example characteristics for the HP40948-3B detector are shown in Figure Current-voltage characteristics measured from the HP40948-3B proximity readout detector at the temperatures of 84 and 90 K. (a) Characteristics measured across the detector. (b) Characteristics measured between the two guard strips when 2000 V was applied across the detector.b. Assuming a detector capacitance of about 10 pF, this sheet resistance gives a characteristic discharge time of about 1 s. This would be the time associated with the dissipation of the charge collected to the proximity surface.

An example of the qualitative radiation response measurements made on the detectors can be found in Figure Induced charge signals measured on the proximity strips of detector 313-3.8. The signals are offset vertically from each other for clarity. The signal from strip 5 is not shown. The signals result from the collection of charge generated by a single gamma-ray interaction event. A Cs-137 source was used.. Shown in this figure are the induced charge signals measured on the proximity strips of one of the detectors. The step change in the signals shown in this figure results from the collection of charge generated by a single gamma-ray interaction event in the detector. Since charge is not completely collected to any one strip, the induced charge is shared between the strips. The strip with the largest step change in signal is the one nearest to the interaction event. For the event of Figure Induced charge signals measured on the proximity strips of detector 313-3.8. The signals are offset vertically from each other for clarity. The signal from strip 5 is not shown. The signals result from the collection of charge generated by a single gamma-ray interaction event. A Cs-137 source was used., the location is between strips 1 and 2, though nearer to strip 2. The inherent sharing of the induced charge among the readout strips in the proximity readout technique allows for a position determination finer than the strip spacing. This will be demonstrated in the next section.

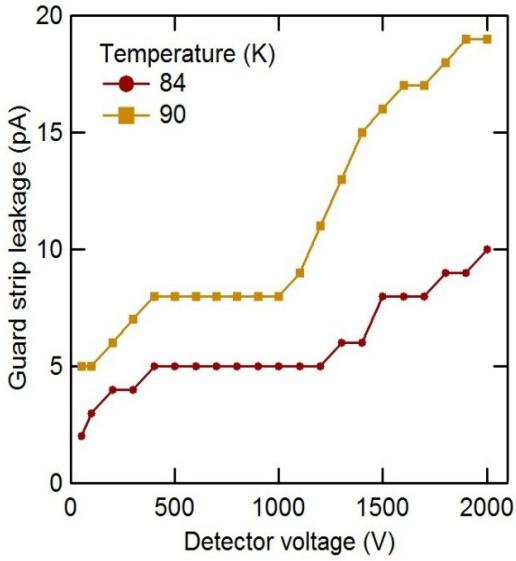

(b)

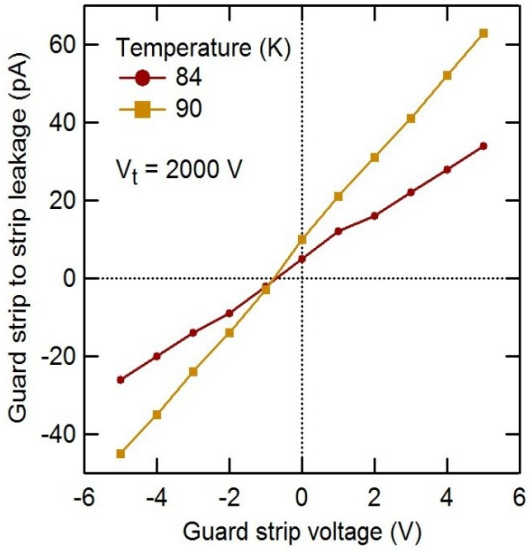

Figure Current-voltage characteristics measured from the HP40948-3B proximity readout detector at the temperatures of 84 and 90 K. (a) Characteristics measured across the detector. (b) Characteristics measured between the two guard strips when 2000 V was applied across the detector.

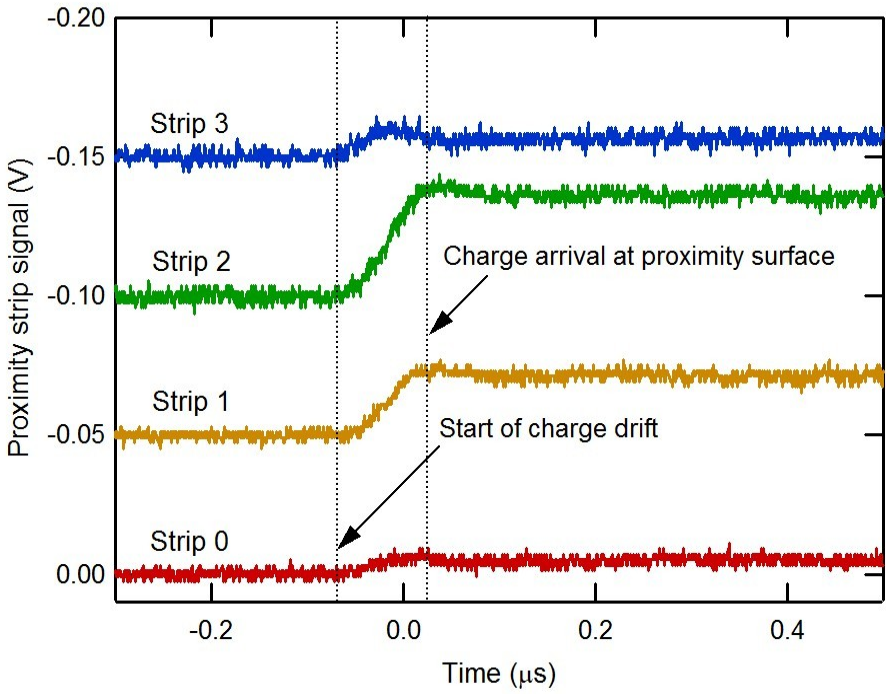

Figure Induced charge signals measured on the proximity strips of detector 313-3.8. The signals are offset vertically from each other for clarity. The signal from strip 5 is not shown. The signals result from the collection of charge generated by a single gamma-ray interaction event. A Cs-137 source was used.

Objective 5: Detailed characterization and data analysis

The goal of this task was to perform detailed radiation response measurements with the proximity readout detectors, analyze the acquired data, and demonstrate gamma-ray interaction event position and energy determination. With the proximity readout technique, the energy is not directly measured and instead must be reconstructed from the pulse height information measured by multiple proximity strips. Furthermore, to obtain event position data finer than the strip spacing, interpolation or other data processing must be applied. Different energy and position reconstruction approaches are possible. For this initial work, we made use of two relatively straight forward approaches that are described below. During the next phase of the program, we plan to more fully study and optimize reconstruction methods. In the following paragraphs, we summarize our measurements, data analysis, and results obtained using two small prototype proximity readout detectors.

Both the HP40948-3B and 313-3.8 proximity detectors were studied. The radiation sources used for the measurements included Co-57 with prominent gamma-ray energies at 122.1 and 136.5 keV and Am-241 with a prominent emission at 59.5 keV. Both uncollimated and collimated source configurations were used. The measurements typically consisted of exposing the detector to a source and acquiring pulse height event data sets using the Pixie electronics. The electronics were configured so that a signal surpassing a set threshold on any one proximity strip would cause the capture of event data from all strips. Though the electronics are capable of capturing pulse height, event time, and digitized pulse shape, our simple analysis methods only required the use of the pulse height data.

One of the simplest methods to assess the measured pulse height data is to generate pulse height histograms for each strip channel. In a conventional detector, such histograms would be energy spectra, but with the proximity detectors this is not the case since the charge is not completely collected to the strips. The energy instead must be reconstructed from the pulse height data. However, through a simple model of the detector, the expected pulse height histograms can be determined and qualitatively compared to the measurements. The model makes use of the weighting potentials of the proximity strips. A weighting potential for an electrode is a mathematical construct that allows one to determine the amount of charge induced on the electrode by a charge exterior to the electrode. The weighting potential of an electrode is the electrostatic potential calculated with the electrode at unity potential, all other electrodes at ground potential, and all space charge removed. The induced charge on the electrode resulting from a nearby point charge is simply the negative of the charge on the point charge multiplied by the weighting potential value at the point charge location. The weighting potentials for all five strips of the small proximity detector calculated at the proximity surface are shown in Figure .

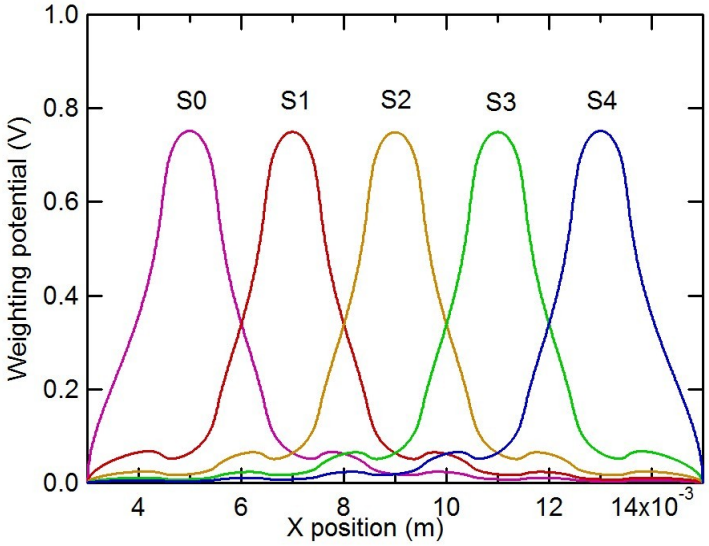

Figure Proximity strip weighting potentials calculated for the geometry shown in Error: Reference source not foundb and described in the Task 3 section. The potentials have been calculated for a line along the proximity surface that is perpendicular to the strips.

From the weighting potentials, the induced charge pulse heights measured by the strips, when the charge from a single gamma event is collected, can be determined by assuming that the charge is point like and fully collected (both electrons and holes) to either the proximity surface or the high voltage electrical contact. Under these assumptions, the charge pulse height will be the amount of charge collected to the proximity surface multiplied by the weighting potential at the location on the surface where the charge is collected. Such a calculation has been done for strip number 2 assuming a uniform illumination of the detector with a monoenergetic source. The resultant calculated pulse height histogram is shown in Figure a below. Pulse height histograms measured from strips 1 through 3 of detector 313-3.8 when illuminated by a collimated Am-241 source centered on strip 2 are shown in Figure b for comparison. The source collimation used was somewhat broad and likely had a FWHM width comparable to the strip pitch of 2 mm.

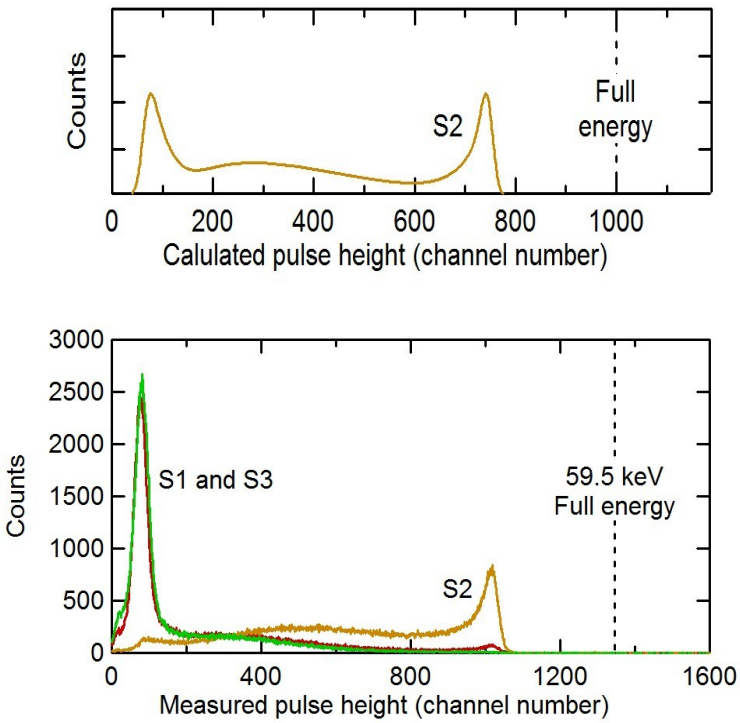

Figure (a) Calculated pulse height histogram from strip 2 assuming flood illumination from a monoenergetic source. The calculation included noise broadening equivalent to 1.5 keV FWHM assuming a 59.5 keV gamma ray source. (b) Measured pulse height spectra from strips 1 through 3 on detector 313-3.8 when illuminated by a collimated Am-241 source centered on strip 2.

In Figure we see that there is good qualitative agreement between the calculated and measured strip 2 pulse height histograms. The histograms do significantly differ at smaller pulse heights, but this is expected since the measurement used a collimated source rather than the flood source assumed in the calculation. The collimation would tend to reduce the number of events far from the strip. These events, since they are not near the strip, only induce a small amount of charge and therefore produce small pulse heights. The measured histograms from strips 1 and 3 are a good demonstration of this in that most of the pulse heights from these strips are small since the source is positioned a distance away from them.

Coarse position determination is straight forward in the proximity strip detectors. The location of a gamma interaction event to within a strip pitch is given by the strip with the largest measured pulse height. For the event shown in Figure Induced charge signals measured on the proximity strips of detector 313-3.8. The signals are offset vertically from each other for clarity. The signal from strip 5 is not shown. The signals result from the collection of charge generated by a single gamma-ray interaction event. A Cs-137 source was used., we can conclude that the location was closest to strip 2. However, since in proximity readout detectors the signal is significantly shared among the strips, a more accurate position determination can be made by comparing signals on nearby strips. Qualitatively, we can conclude from the Figure Induced charge signals measured on the proximity strips of detector 313-3.8. The signals are offset vertically from each other for clarity. The signal from strip 5 is not shown. The signals result from the collection of charge generated by a single gamma-ray interaction event. A Cs-137 source was used. signals that the event must have

occurred between strips 1 and 2, and that it was slightly closer to 2 than to 1. To determine the position more accurately, we can calculate or reconstruct the position from the measured pulse heights. We have looked at two different reconstruction methods. In a simple method, we assume that the detector geometry is accurately known, calculate the weighting potentials of the proximity strips (as was done to generate the potentials of Figure), and determine the position based on the measured pulse heights and the calculated weighting potentials. Once this is done the gamma ray energy can be determined based on the extracted position, weighting potentials at that position, and the measured pulse heights. In the second method, the weighting potentials are determined from flood illumination event data and the requirement that the position distribution be uniform. Once the weighting potentials are known, position and energy reconstruction can be done as described in the first method.

Preliminary position reconstruction from a linear scan of detector 313-3.8 using the second method is shown in Figure . The source was Am-241 collimated to about 2 mm FWHM. Reconstruction was done for events with positions between 8 and 10 mm. The solid lines in the figure give the presumed event distribution at each of the five source locations, and the circles are the position histogram data points reconstructed from the measured pulse height data. The position histograms show the beam profile of the source as it is scanned under strip 2. The positional accuracy is clearly much better than that of the strip pitch. This then demonstrates one of the significant advantages of the proximity approach.

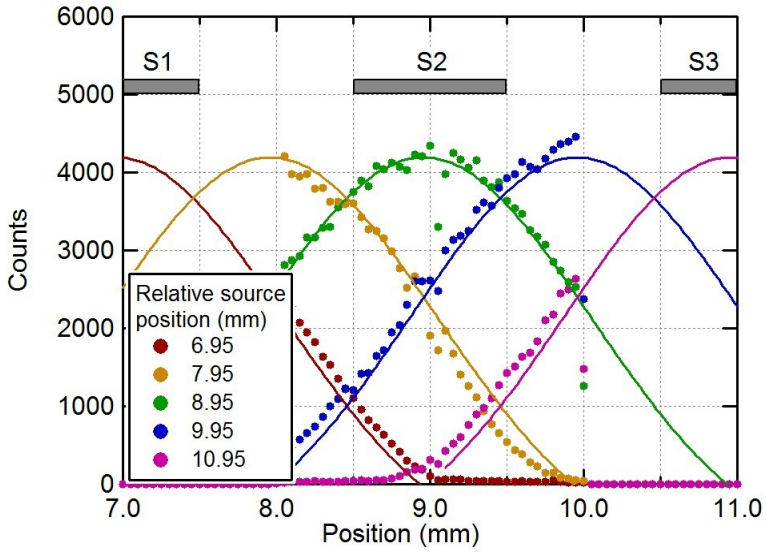

Figure Gamma-ray event position histograms reconstructed from data acquired with detector 313-3.8. The source used was Am-241 collimated to about 2 mm FWHM. Data sets were acquired at five different source locations. The solid lines give the presumed source distribution at each source location, and the circles are the reconstructed histograms at those locations. The reconstruction was only done for events between 8 and 10 mm.

To complete the analysis of the proximity data, the energy of each event must be determined. Once the event position has been determined, the energy can simply be calculated using the weighting potential and pulse height from the strip nearest to the event, and a previously determined energy calibration. Example reconstructed energy spectra are given in Figure . These energy spectra illustrate that the full energy can be recovered through reconstruction, but do not illustrate the energy resolution potential of the approach since they were obtained from prototype

detectors and simple reconstruction methods were employed. Many factors affect the energy resolution including proximity surface coating, proximity surface flatness, proximity electrode uniformity, and reconstruction method. In Phase II of this program, we plan to study these factors, optimize the detector and reconstruction methods, and demonstrate the position and energy resolution potential of the proximity readout approach.

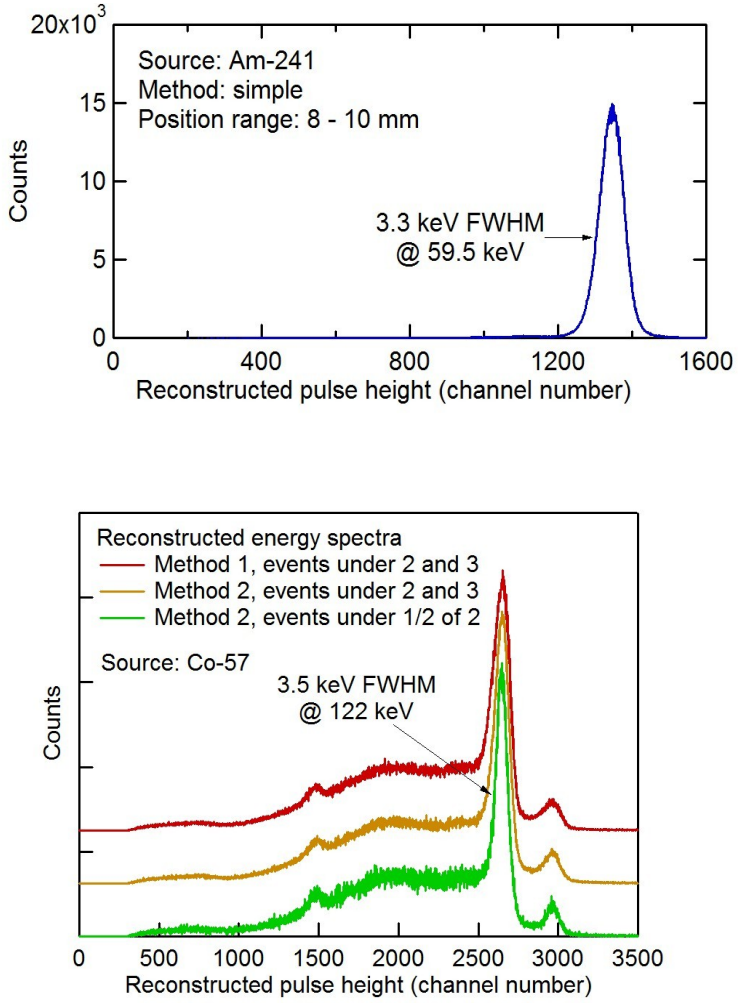

Figure (a) Am-241 energy spectrum reconstructed from data acquired with detector 313-3.8. The reconstruction was only done for events between 8 and 10 mm, and the simple reconstruction method was used. (b) Co-57 energy spectra reconstructed from data acquired with detector HP40948-3B. The reconstruction was done using both the simple method (method 1) and the more complex method 2. The spectra are offset vertically for clarity and normalized. The energy resolutions from the top to the bottom spectrum are 5.1, 4.6, and 3.5 keV FWHM. Substantial background from scattering exists in the Co-57 spectra as a result of a very thick Al entrance window. This window was substantially reduced prior to the measurements made with the Am-241 source and detector 313-3.8.

In conclusion, all aspects of the Phase I program were successfully completed, and a clear demonstration of the proximity approach, as applied to HpGe, was made. In Phase II we propose to build a prototype large-area SD, identify and improve on limitations in the existing processes by evaluating its performance through test measurements and quantitative spectrum analysis. The multi-strip remote sensing boards will be readout by new XIA high-channel, low-cost electronics with firmware and software upgrades to perform on-board pulse shape discrimination, position and time resolution.